

## Article

# A Multi-Enzyme Cascade for the Production of High-Value Aromatic Compounds

Claudia Engelmann <sup>1</sup>, Jens Johannsen <sup>2</sup> , Thomas Waluga <sup>2</sup>, Georg Fieg <sup>2</sup>, Andreas Liese <sup>1</sup>   
and Paul Bubenheim <sup>1,\*</sup> 

<sup>1</sup> Institute of Technical Biocatalysis, Hamburg University of Technology, Denickestr. 15, 21073 Hamburg, Germany; claudia.engelmann@tuhh.de (C.E.); liese@tuhh.de (A.L.)

<sup>2</sup> Institute of Process and Plant Engineering, Hamburg University of Technology, Am Schwarzenberg-Campus 4, 21073 Hamburg, Germany; jens.johannsen@tuhh.de (J.J.); thomas.waluga@tuhh.de (T.W.); g.fieg@tuhh.de (G.F.)

\* Correspondence: paul.bubenheim@tuhh.de

Received: 29 September 2020; Accepted: 15 October 2020; Published: 20 October 2020



**Abstract:** Cascade reactions are the basis of life in nature and are adapted to research and industry in an increasing manner. The focus of this study is the production of the high-value aromatic ester cinnamyl cinnamate, which can be applied in flavors and fragrances. A three-enzyme cascade was established to realize the synthesis, starting from the corresponding aldehyde with in situ cofactor regeneration in a two-phase system. After characterization of the enzymes, a screening with different organic solvents was carried out, whereby xylene was found to be the most suitable solvent for the second phase. The reaction stability of the formate dehydrogenase (FDH) from *Candida boidinii* is the limiting step during cofactor regeneration. However, the applied enzyme cascade showed an overall yield of 54%. After successful application on lab scale, the limitation by the FDH was overcome by immobilization of the enzymes and an optimized downstream process, transferring the cascade into a miniplant. The upscaling resulted in an increased yield for the esterification, as well as overall yields of 37%.

**Keywords:** enzyme cascade; aromatic compounds; esterification; scale-up; continuous reactor operation; immobilization

## 1. Introduction

Based on a long history, e.g., beer brewing or cheese fermentation, biocatalysis is a highly important method in industry. Thereby, biocatalytic cascades play a fundamental role in nature and in biotechnology where they show great advantages, such as environmental friendliness, less intermediate separation, and more sustainable reactions due to less byproduct formation. Different methods are used to improve the productivity of biotechnological processes, whereby the cores of research are an efficient cofactor regeneration and the downstream processing [1,2]. Especially the enzyme group of oxidoreductases require cofactors, which are often very cost intensive, constituting the need for their regeneration. This is often realized by using a second enzymatic reaction, since enzymes are highly selective and efficient. Important applications for cofactor regeneration are, e.g., the synthesis of chiral alcohols by the reduction in prochiral ketons via ketoreductases with an integrated cofactor regeneration by a glucose dehydrogenase [3].

In this study, an enzymatic cascade is established, applying a bi-phasic system and integrated cofactor regeneration, shown in Figure 1. A high-value ester is synthesized, which can be used in fragrances and flavors such as odors, blending agents, or non-musk fixatives, applying an enzyme cascade with three different biocatalysts [4]. The reaction starts from cinnamyl aldehyde, available

from natural resources. The aldehyde is reduced by an alcohol dehydrogenase (ADH) to the corresponding alcohol in an aqueous phase, utilizing nicotinamide adenine dinucleotide (NADH) as cofactor. In parallel, an FDH is applied for in situ cofactor regeneration. This regeneration has the advantage that it is an almost irreversible reaction and the product  $\text{CO}_2$  is bound in the aqueous phase [5]. Subsequently, the produced alcohol is extracted by the second, organic phase, and esterified with cinnamic acid to obtain the desired ester cinnamyl cinnamate, catalyzed by a lipase. Therefore, the enzymes are characterized regarding their kinetics, an organic solvent as second phase is selected and investigated to obtain a suitable reaction system. The overall aim was to realize the whole cascade in two reaction steps with in situ extraction and subsequent scale up into a miniplant, based on these investigations. This cascade reaction system can also be applied for syntheses of further esters, utilizing aldehydes as substrates.

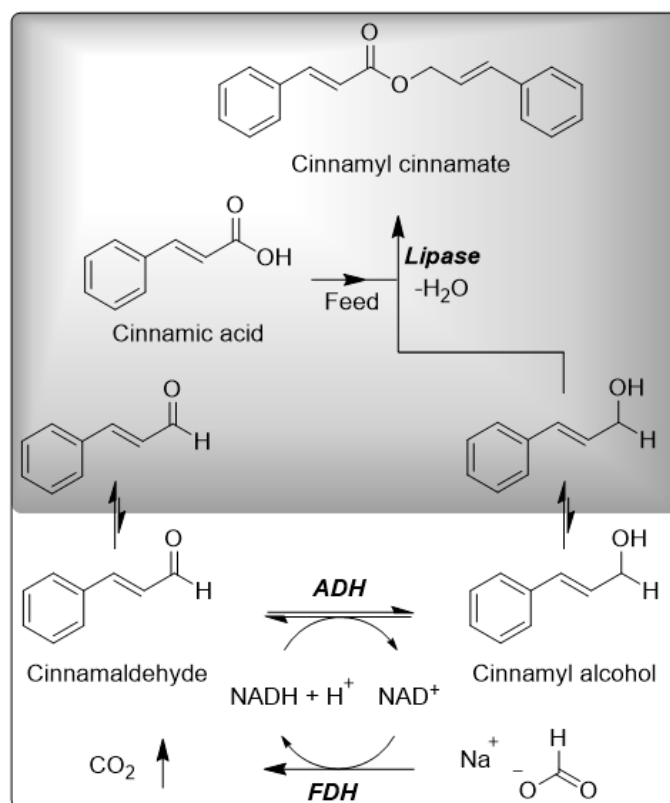


Figure 1. Reaction scheme of the multienzyme cascade.

## 2. Results

### 2.1. Enzyme Characteristics

For an effective cascade reaction system, a suitable alcohol dehydrogenase and different immobilized lipases were screened regarding the applied substrates. For the lipase, the immobilized preparation Novozym<sup>®</sup>435 showed one of the highest activities, and since it is commercially available, it was chosen for the reaction system (see Supplementary Materials). Different alcohol dehydrogenases were screened, whereby only three showed activity regarding the cinnamyl aldehyde and the highest activity was obtained with the enzyme ADH97L (c-LEcta, Leipzig, Germany) (further details in Supplementary Materials). Furthermore, this enzyme showed activities up to a pH of 8.5 and 2.5% higher activities at high temperatures up to 60 °C (further details in Supplementary Materials). For cofactor regeneration in the aqueous phase, FDH from *Candida boidinii* was used, due to its availability and efficiency for cofactor regeneration [6–10]. The implementation of the two different

enzymes requires a maximum pH value to perform the reduction with in situ cofactor regeneration. The applied FDH has a comparable broad pH range (pH 5–11) whereby the optimum of the ADH97L is at pH 7 [11]. As a compromise regarding the cofactor regeneration, a pH value of 8 was selected for the presented system.

The kinetic parameters based on reaction rate measurements of the enzymes are presented in Table 1. For the ADH and FDH a two-substrate kinetic with product inhibition, cf. Equation (2) (Section 4.2), was calculated via the Michaelis–Menten equation with MATLAB R2018b. The applied ADH was an overexpressed enzyme, with  $K_M$  values of 0.39 mM for the aldehyde and 0.08 mM for NADH. In literature, values for cinnamyl aldehyde reduction by ADHs range from 0.009–0.1 mM, presenting a higher substrate affinity compared to the present study. In literature,  $K_M$  values for NADH from 0.025–0.177 mM were found, so that the utilized ADH97L showed a comparable high affinity [12–15]. However, different ADHs showed a broad activity range for cinnamyl aldehyde reduction of  $3.9 \times 10^{-3}$  U–14.4 U, [13] whereby with the applied ADH97L a value of 3.5 U was obtained, which is within the literature range. In addition, a product inhibition by cinnamyl alcohol was found for the ADH97L with a comparable low  $K_I$  of 0.04 mM. In literature, inhibitions of ADHs by substrates or products are described, but no data are available for the investigated substrate and reaction system [16,17]. In comparison to this specific ADH, the FDH from *Candidia boidinii* is well-studied and used in industry for cofactor regeneration, e.g., in reductive amination. [18]  $K_M$  values obtained during these investigations were with 10.14 mM (formate) and 0.04 mM ( $\text{NAD}^+$ ) in the range of the data, which can be found in literature presenting values for formate between 4–20 mM and for  $\text{NAD}^+$  from 50–90  $\mu\text{M}$  [19–21].

**Table 1.** Kinetic data of the enzymes used in the cascade (further details see supplementary materials).

Enzyme	$v_{max,f}$	$v_{max,b}$	$K_{M,S1}^{[a]}$	$K_{M,S2}^{[a]}$	$K_{M,P1}^{[b]}$	$K_{M,P2}^{[b]}$	$K_I^{[c]}$	$k_{cat}^{[d]}$
ADH [e]	3.49 U/mg $\pm$ 1.53	n.e.[g]	CA 0.39 mM $\pm$ 0.20	NADH 0.08 mM $\pm$ 0.07	n.e. [g]	n.e. [g]	CAI 0.04 mM $\pm$ 0.3	1.6 s <sup>−1</sup>
FDH [e]	0.46 U/mg $\pm$ 0.07	n.e.[g]	NF 10.14 mM $\pm$ 6.67	NAD <sup>+</sup> 0.04 mM $\pm$ 0.02	n.e. [g]	n.e. [g]	NADH 0.27 mM $\pm$ 0.42	8.1 s <sup>−1</sup>
Lipase [f]	6.31 U/g $\pm$ 1.19	14.75 U/g $\pm$ 2.79	CAI 2.77 mM $\pm$ 0.52	CAC 1.40 mM $\pm$ 0.27	CC 0.78 mM $\pm$ 0.15	H <sub>2</sub> O 252.89 mM $\pm$ 47.86	CAC 13.72 mM $\pm$ 2.60	3500 s <sup>−1</sup>

[a]  $K_M$  of the substrates. [b]  $K_M$  values of the back reaction. [c] Inhibition constants: competitive inhibition in the case of ADH and FDH and non-competitive inhibition of the lipase. [d] Calculated for enzyme preparation. [e] Calculated with MATLAB R2018b. [f] Calculated with Encora 1.2. [g] n.d.—not detectable. CA—cinnamyl aldehyde, Cal—cinnamyl alcohol, CAC—cinnamic acid, CC—cinnamyl cinnamate. Cond.: ADH/FDH: phosphate buffer, 0.1 M, pH 8,  $c_{\text{cinnamyl aldehyde}} = 0.01\text{--}5$  mM,  $c_{\text{NADH}} = 0.005\text{--}0.15$  mM,  $c_{\text{Na formate}} = 2.5\text{--}300$  mM,  $c_{\text{NAD}^+} = 0.02\text{--}1$  mM,  $\lambda = 360$  nm,  $T = 30$  °C. Lipase:  $V_{\text{Xylene}} = 50$  mL,  $c_{\text{cinnamyl alcohol}} = 10\text{--}80$  mM,  $c_{\text{cinnamic acid}} = 5\text{--}60$  mM,  $m_{\text{Lipase}} = 2$  g,  $T = 60$  °C under reflux conditions.

Regarding the applied lipase, Novozym®435, various kinetic models are described in literature [22–31]. For this study, forward and backward reactions as well as substrate inhibition by cinnamic acid were assumed, due to the high concentration in the organic phase on the miniplant of up to 100 mM. In addition, substrate dissociation constants for the forward and backward reactions were considered. Further inhibitions were not considered, due to the low solubility of the compounds in the aqueous phase and therefore low concentration after extraction into the organic phase. This leads to Equation (1):

$$v = \frac{v_{max,f} \cdot \left( c_{CAI} \cdot c_{CAC} - \frac{c_{CC} \cdot c_{H_2O}}{K_{eq}} \right)}{K_{i,CAC} \cdot K_{M,Al} + K_{M,Ac} \cdot c_{CAC} \left( 1 + \frac{c_{CAC}}{K'_{i,CAC}} \right) + K_{M,CAC} \cdot c_{CAI} + \frac{v_{max,f}}{v_{max,b}} \cdot \frac{K_{M,H_2O} \cdot c_{CC}}{K_{eq}} + \frac{v_{max,f}}{v_{max,b}} \cdot \frac{K_{M,CC} \cdot c_{H_2O}}{K_{eq}} + c_{CAC} \cdot c_{CAI} + \frac{v_{max,f}}{v_{max,b}} \cdot \frac{c_{CC} \cdot c_{H_2O}}{K_{eq}}} \quad (1)$$

with  $K_{eq} = v_{max,f} \cdot K_{i,H_2O} \cdot K_{M,CC} / (v_{max,b} \cdot K_{i,Ac} \cdot K_{M,Al})$ .

The kinetic parameters were calculated via progress curve analysis, whereby three esterifications with different starting concentrations were analyzed using the software Encora 1.2 [32]. The standard deviations of kinetic parameters were calculated via residual variance according to Duggleby [33].

In Table 1, the calculated values are shown, whereby the kinetic values of the applied lipase in literature show a broad range of activity. However, in literature, the esterification and transesterification are only carried out with cinnamic acid or the corresponding alcohol, so that no comparison can be made [34,35].

## 2.2. Solvent Screening

The enzyme cascade was to be applied in a two-step reaction system with in situ extraction for the second reaction step. Different organic solvents were investigated regarding their hazardous nature and suitability regarding the scale-up; results are shown in Table 2. Alfonsi et al. developed a solvent guide for medical chemistry, whereby the solvents were assessed in workers safety, process safety, and environmental and regulatory considerations. This assessment was used in the present study to find a suitable organic solvent, whereby all selected organic solvents were usable for the application with logP values ranging from 0.84 to 3.58, except diethyl ether. However, most usable organic solvents listed by Alfonsi et al. were not suitable for application in the cascade reaction system, since they were water-soluble or presenting possible substrates for the applied enzymes. Due to the miniplant, a classification was carried out regarding the suitability of the organic solvent for the up-scaling. The compounds were categorized in four classes from *a* to *d*, whereby diethyl ether does not show suitable properties similar to the consideration of the hazardous nature described in literature, as well as toluene [36]. The best results regarding the suitability in a larger plant were obtained with xylene, cyclopentylmethyl ether (CPME), and methyl-*tert*-butyl ether (MTBE).

**Table 2.** Assessment of organic solvents.

Solvent	logP <sup>1</sup>	Boiling Point <sup>2</sup>	Hazardous Nature (Pfizer) <sup>3</sup>	Miniplant Suitability <sup>4</sup>
Heptane	3.58	98 °C	2	c
Isooctane	3.56	99 °C	2	c
<i>p</i> -Xylene	3.00	138 °C	2	a
Cyclohexane	2.67	84 °C	2	c
Toluene	2.49	111 °C	2	d
Cyclopentylmethyl ether	1.48	106 °C	- <sup>5</sup>	a
Methyl- <i>tert</i> -butyl ether	1.18	55 °C	2	a
2-Methyltetrahydrofuran	0.95	80 °C	2	b
Diethyl ether	0.84	35 °C	3	d

<sup>1</sup> Calculated online by chemicalize.com. <sup>2</sup> Sigma Aldrich 10.09.20. <sup>3</sup> Assessment by Alfonsi et al. at Pfizer: 1—preferred, 2—usable, 3—undesirable. <sup>4</sup> Suitability for the scale-up in the miniplant: a—preferred, b—ok, c—usable, d—undesirable. <sup>5</sup> No reference.

In the continuous cascade system, an equilibrium of water and organic solvent between the two phases will always be present. This results in a partly dissolution of the organic solvent in the aqueous phase and vice versa, which can have a direct influence on the enzyme activity [37,38]. For a better understanding of this effect, the retained enzyme activity was investigated by saturating the aqueous buffer phase with the used organic solvent. Subsequently, the reduction in cinnamyl aldehyde by the ADH was investigated. It can be seen that the kinetics carried out with the selected organic solvents show a similar course with significant differences regarding the residual activities under the given conditions (further details in Supplementary Materials). In Figure 2, the retained apparent maximum reaction rate is plotted against the logP values of the applied organic solvents. With low logP values, a very low residual activity of the ADH was measured, which was decreasing further up to a logP of 1.48 (CPME) presenting the lowest activity. With an increasing logP value, the residual activity is significantly increasing, whereby the best results with 91.3% residual activity were obtained using isooctane and heptane, offering the highest logP values. The low influence on enzyme activity using solvents with a high logP value in two-phase systems is described by different research groups; however, in literature, an S-shape curve is described, whereby with low hydrophobicities almost no detectable activity is described [39–41]. In contrast, the measurements carried out during this study showed a

minimum activity at logP 1.48 (CPME) and increasing activities with further decreasing logP values. This behavior is based on the nature of the enzyme, e.g., the different active centers, and was observed also during the studies of Cantarella and co-workers, who obtained a significant difference in solvent dependence in comparison to the description of Grundtvig et al. The results highlight that the influence of the organic solvents has always to be tested for the specific application [40,42]. The substrates applied during this study showed a low solubility in isooctane and heptane but showed high residual activities in the enzyme reaction. The solubility in xylene was comparably high, which could be based on the aromatic structure of the substrate and a high residual enzyme activity was found as well, so that xylene was chosen as an organic solvent for the study.

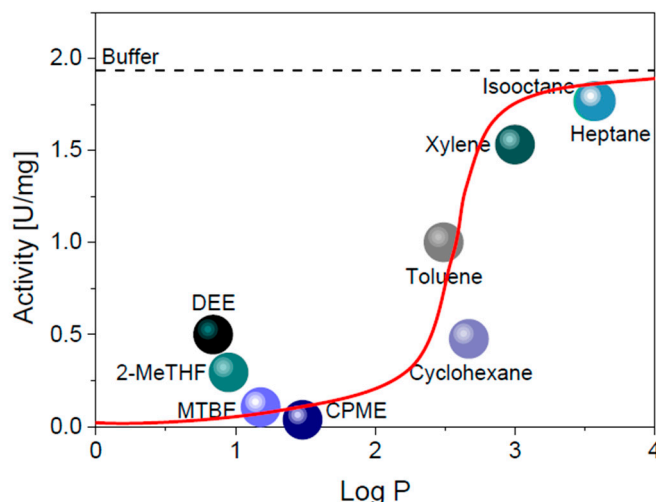


**Figure 2.** Solvent screening regarding residual enzyme activity. Solid line: in literature, described influence of LogP value on enzyme activity. [40] Dashed line: enzyme activity in buffer without organic solvent. Conditions: with organic solvent saturated Tris-HCl buffer (pH 7, 0.1 M, 2 mM  $\text{MgCl}_2$ ),  $c_{\text{cinnamyl aldehyde}} = 0.1\text{--}6$  mM,  $m_{\text{ADH}} = 0.1$  mg,  $c_{\text{NADH}} = 0.1$  mM,  $\lambda = 360$  nm,  $30^\circ\text{C}$ .

### 2.3. Reaction in the Aqueous Phase

For evaluation of the complete reaction system, the establishment of the in situ cofactor regeneration had to be realized. Therefore, the FDH from *Candida boidinii* was chosen, since formate is a cheap hydrogen source and not extracted in the organic phase during the downstream processing under the chosen conditions. In addition,  $\text{CO}_2$  as a reaction product dissolves in the aqueous phase [43]. In Figure 3, the reaction progress in the aqueous phase is shown by plotting the amount of cinnamyl aldehyde and cinnamyl alcohol over time. A complete conversion was reached with a yield of 100%. Since  $\text{CO}_2$  could change the pH value caused by dissolution in water and combined with subsequent in situ formation of carbonic acid, the pH value was tracked during the course of the reaction. However, no change was observed, so that the buffer concentration is sufficient for the applied reaction conditions. Nevertheless, in a continuous process with a substrate feed, the concentration of the buffer should be high enough to compensate the produced  $\text{CO}_2$ . It can be dissolved until 70 mM in pure water and shows a decreasing solubility with salt addition; therefore, the buffer was used at a concentration of 100 mM [44].

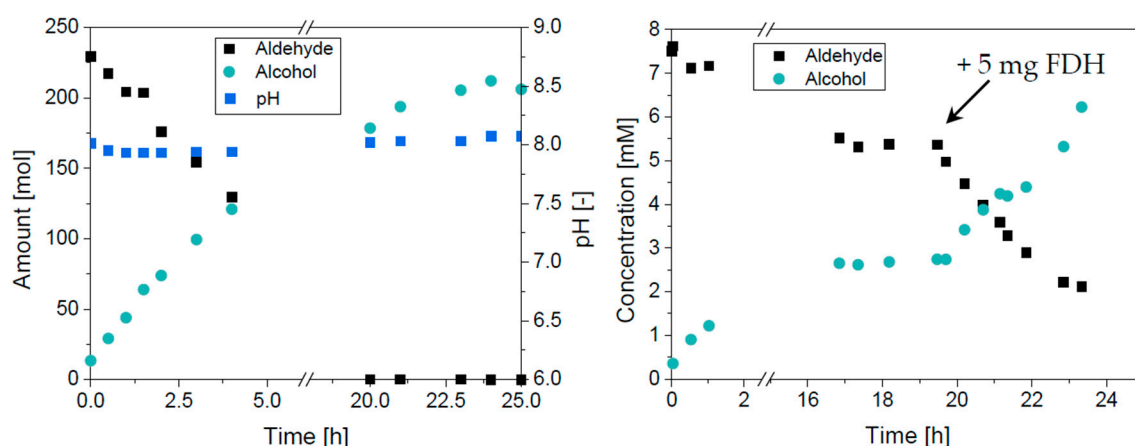


**Figure 3.** Reaction progress of the aqueous phase with in situ cofactor regeneration. Conditions: left: potassium phosphate buffer pH 8, 0.1 M,  $V = 25$  mL,  $c_{\text{Aldehyde}} = 7.5$  mM (fed with 0.3 mL/h),  $c_{\text{NADH}} = 0.1$  mM,  $m_{\text{ADH}} = 3,125$  mg,  $m_{\text{FDH}} = 5$  mg,  $c_{\text{sodium formate}} = 200$  mM,  $30$  °C. Right: potassium phosphate buffer pH 8, 0.1 M,  $V = 25$  mL,  $c_{\text{Aldehyde}} = 7.5$  mM,  $c_{\text{NADH}} = 0.15$  mM,  $m_{\text{ADH}} = 0.5$  mg,  $m_{\text{FDH}} = 5$  mg,  $c_{\text{sodium formate}} = 100$  mM,  $30$  °C.

Adding more substrate, it became clear that the FDH is crucial for the system to sustain the cofactor regeneration, limiting the conversion of the ADH. The resulting incomplete conversion of the substrate could be overcome by adding more FDH to the system, see Figure 3, right.

The deactivation of the FDH in the cascade was investigated in detail with differential scanning fluorimetry technology [45,46]. The protein stability is determined by measuring the intrinsic fluorescence (NanoTemper Technologies GmbH, Munich, Germany) of the protein based on its folding state. In Figure 4, the scanning results are shown; however, only FDH could be tracked with this technique based on visible amino acid residues in comparison to the ADH. It can be seen that the measurement of the reaction mixture resulted in a slight shift of the single peak, presenting the FDH, which shows the influence of the other reaction compounds (further details in Supplementary Materials). This method was applied for the investigation of the FDH stability, plotted in Figure 4b. A continuous decrease in the flexibility, folding, and unfolding occurred, indicating a deactivation of the FDH over the reaction progress. Since the storage stability of the enzyme is comparably high (over 160 h) [47], these results indicate that the FDH is deactivated by the reaction itself. A possibility for the deactivation could be microemulsions, which is a phenomenon described in literature. Orlich et al. detected only up to 2.5% residual activity with those emulsions based on application of hydrophobic substrates and products [48]. However, Gröger et al. observed a significant deactivation by non-polar aromatic hydrocarbons applying 10% (*v/v*) in the reaction. During the present study, 0.06% (*v/v*) of the substrate was used, so that this effect should be comparably low [48,49]. In addition, an increasing amount of ADH resulted in a faster decrease in FDH stability, which underlines the effect of deactivation by the reaction itself and increasing conversion by the FDH in parallel. (SI) A further reason for the deactivation could be orthokinetic flocculation by contact between the particles based on the agitation of the bulk medium presenting a general problem in biocatalytic reactions [46].

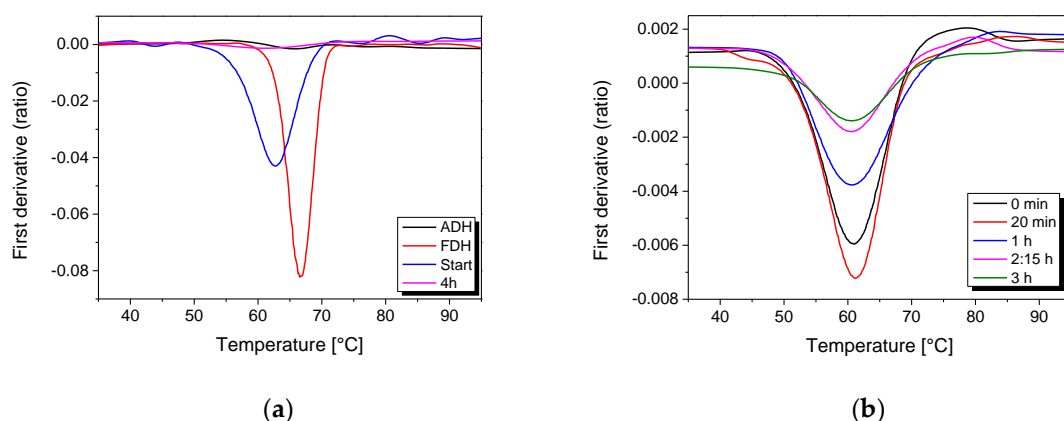


**Figure 4.** Measurement of protein stability by differential scanning fluorimetry. (a) Crude enzymes in comparison to start and end point of a reaction. (b) Reaction progress over 3 h. Conditions: potassium phosphate buffer pH 8, 0.1 M,  $V = 25$  mL,  $c_{\text{Aldehyde}} = 7.5$  mM,  $c_{\text{NADH}} = 0.15$  mM,  $m_{\text{ADH}} = 0.5$  mg,  $m_{\text{FDH}} = 5$  mg,  $c_{\text{sodium formate}} = 100$  mM,  $30$  °C.

#### 2.4. Application of the Enzyme Cascade

Finally, the whole cascade was operated batchwise via the two-step synthesis. The reduction in cinnamyl aldehyde was realized in one pot, and after extraction, the esterification was performed at  $60$  °C under reflux conditions. As can be seen in Figure 5, in the first step of the cascade, full conversion of the substrate was reached, yielding in 96% of cinnamyl alcohol after 4 h. During the esterification, the second step, a conversion of about 90% was obtained with a high product yield of 50%. Here, limitations for the esterification became visible, whereby one reason is the thermodynamic limitation of the reaction based on especially the presence of the side-product water. In addition, further side products can reduce the yield for the ester, so that only 50% could be reached. Another problem could be an evaporation of the alcohol despite the application of the reflux condenser and a comparably low solubility of the acid in the reaction mixture, whereby partly a precipitation at the surface or between the two phases was visible.

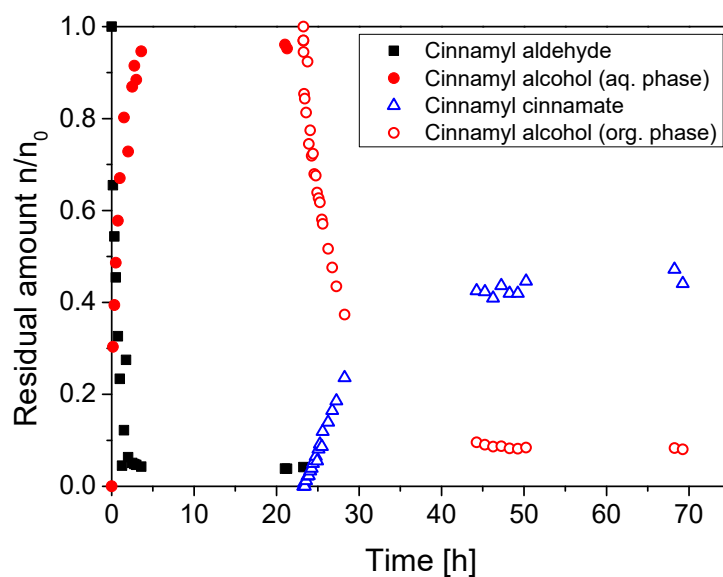


**Figure 5.** Lab-scale application of the cascade reaction. Conditions: aqueous phase: potassium phosphate buffer pH 8, 0.1 M,  $V = 25$  mL,  $c_{\text{Aldehyde}} = 4$  mM,  $c_{\text{NADH}} = 1$  mM,  $m_{\text{ADH}} = 2$  mg,  $m_{\text{FDH}} = 5$  mg,  $c_{\text{sodium formate}} = 100$  mM,  $30$  °C; organic phase: 25 mL xylene with extracted alcohol,  $c_{\text{Acid}} = 3.4$  mM,  $m_{\text{Lipase}} = 1$  g, 3.3 g molecular sieve,  $60$  °C.

After the detailed investigation and characterization of the cascade on lab scale, the cascade was implemented on a larger scale by our project partners in the miniplant; for details, see Johannsen et al. [50]. With this set-up, an in situ extraction with an extraction centrifuge after the first reaction step in aqueous media could be realized, enabling a subsequent esterification in a packed-bed reactor (PBR) with xylene as a solvent. In the miniplant, a rotating bed reactor containing the previously described immobilized enzymes is used for the reaction in the aqueous phase. ADH and the FDH were covalently immobilized onto porous silica particles, with a previous published method [51]. The scale-up of the cascade into an 800 mL miniplant-scale (aqueous phase) reactor resulted in a lower conversion compared to the lab-scale reaction (25 mL) of around 50% for the first step (shown in Figure 6). However, the reaction equilibrium was not reached, so that a higher conversion needs possibly a longer reaction time or an increased amount of enzyme. The main reason for this lower productivity was the usage of immobilized enzymes, which showed a reduced activity after immobilization. In contrast, esterification after extraction into the organic phase showed a higher yield than in the small scale. An explanation could be a lowered film diffusion limitation at the heterogenous biocatalyst preparation in the fixed bed in contrast to the stirred tank reactor. In addition, a lower starting concentration of water realized by a lower temperature of 10 °C instead of 20 °C, decreasing the water solubility during the extraction, which resulted in increasing productivity of the lipase [50]. However, the overall yield of the lab-scale reaction reached 54%, whereby a yield of 37% was obtained during the scale-up. The results proved that the reaction could be realized; however, there is still room for improvement, especially, for the first reaction step in the aqueous phase using the miniplant: e.g., longer reaction times or increasing enzyme activities. With this, a higher yield of up to 96% for the reduction is possible, as demonstrated at lab scale, and therefore, a higher overall yield could be reached.

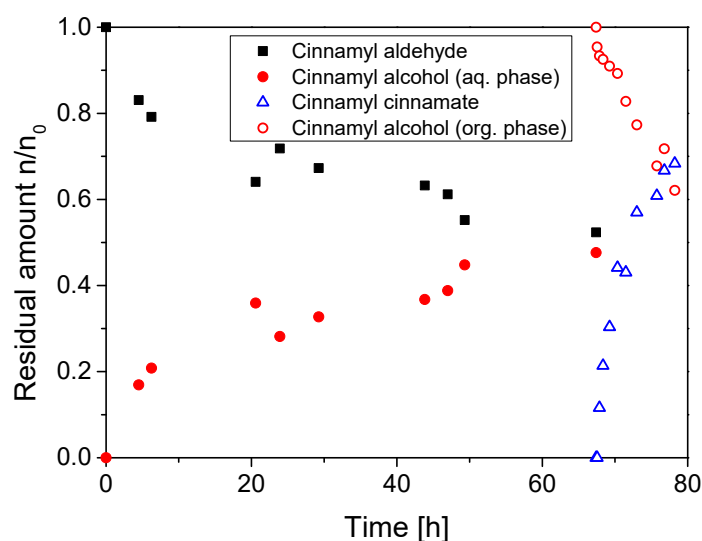


**Figure 6.** Reaction of the applied cascade reaction with immobilized enzymes in the miniplant. Conditions: aqueous phase: potassium phosphate buffer pH 8, 0.1 M,  $V = 0.5$  L,  $c_{\text{Aldehyde}} = 8.8$  mM,  $c_{\text{NADH}} = 3.4$  mM,  $m_{\text{ADH}} = 21.3$  mg,  $m_{\text{FDH}} = 6.6$  mg,  $c_{\text{sodium formate}} = 327.5$  mM, 30 °C; organic Phase: Xylene,  $V = 0.6$  L,  $c_{\text{Acid}} = 56.3$  mM,  $m_{\text{Lipase}} = 12.8$  g, 60 °C.

### 3. Discussion

The cascade reaction system was applied successfully in the lab and subsequently in the miniplant. The enzymes applied in the aqueous phase for the cinnamyl aldehyde reduction, ADH97L and the FDH from *Candida boidinii*, showed comparable kinetics to those described in literature. Only for the lipase, Novozym<sup>®</sup>435, no comparison could be made, since the combination of two comparable large molecules as substrate is not well described in literature. The reason might be that those substrates

lead to a comparable high steric hindrance in the active center of the enzyme, resulting in low enzyme activities. This also emphasizes the uniqueness of this reaction system. Our investigations showed that limitations in the process were caused by the stability of the FDH. This challenge could be overcome by, e.g., protein engineering, enzyme immobilization or the application of a more stable enzyme for cofactor regeneration. The screening of organic solvents, applied as second phase for product extraction, revealed different deactivations of the enzymes in the aqueous phase based on the chemical properties. Xylene showed the best results in retained enzyme activity, with low water solubility as well as high solubility for the other reaction compounds. One reason for this can be the aromatic structure of the compounds, an important aspect for the extraction of cinnamon derivatives and the application in the miniplant system, leaving room for further experiments. Application of the cascade in the miniplant enabled even higher yields for the esterification, which could be based on the usage of the PBR presenting an optimal reaction set-up, due to a more extensive substrate enzyme interaction. The utilization of immobilized enzymes enables furthermore the recycling of the enzymes, so that higher productivities do result in the complete process [51].

With the established three-enzyme cascade reaction and the subsequent downstream processing in a miniplant, ester synthesis was realized. Furthermore, there is still room for improvement presenting an interesting process for the synthesis of flavors and fragrances in industry.

#### 4. Materials and Methods

##### 4.1. Materials

The different alcohol dehydrogenases for the screening were a free sample of c-LEcta (Leipzig, Germany) and the ADH 97L for the application in the process was purchased from c-LEcta. The formate dehydrogenase was purchased from Sigma-Aldrich (Steinheim, Germany).

Sodium formate, cinnamyl aldehyde, cinnamyl aldehyde NAD<sup>+</sup>, NADH, sodium alginate, chitosan, hydrochloric acid, glutaraldehyde, ethanol, heptane, potassium dihydrogen phosphate, and dipotassium hydrogen phosphate were purchased from Roth (Karlsruhe, Germany) and 3-(Aminopropyl)triethoxysilane (APTES), as well as tetraethyl orthosilicate (TEOS) from TCI (Eschborn, Germany).

##### 4.2. Kinetics

The kinetics of the ADH and FDH were determined via initial reaction rate measurements. Different substrate concentrations were measured spectrophotometrically at a defined concentration of the second substrate at a wavelength of 360 nm. For the inhibition, the product concentration was varied and both substrate concentrations were kept constant. The reactions were performed in a potassium phosphate buffer (pH 8, 0.1 M) at 30 °C. Subsequently, the kinetics were calculated with MATLAB R2018b based on Michaelis–Menten two-substrate kinetic with product inhibition by cinnamyl alcohol and NADH, respectively.

$$v = \frac{v_{max} \cdot c_{S1} \cdot c_{S2}}{(K_{M1} + c_{S1}) \cdot \left(K_{M2} + \frac{c_{S2}}{K_{I,S2}}\right)} \quad (2)$$

Equation (1) describes the reaction rate  $v$  depending on the substrate concentration  $c_S$  with the maximum reaction rate  $v_{max}$  and the Michaelis–Menten constants  $K_M$  for the two substrates.

The kinetics of the lipase were calculated with Encora 1.2, based on three esterifications with different starting concentrations, which reached the reaction equilibrium.

##### 4.3. Solvent Screening

For the screening of the organic solvents, 50 mL potassium phosphate buffer (pH 8, 0.1 mM) were saturated with 20 mL of the organic solvent. Therefore, the two phases were mixed vigorously with a vortex and allowed to settle. After separation of the two phases, the lower aqueous phase was

transferred into a closed bottle for easier handling. With this, the initial reaction rate using different concentrations of cinnamyl alcohol by the ADH were measured spectrophotometrically at 360 nm and 30 °C. The results were plotted and the occurring activities using different organic solvents compared, depending on their hydrophobicity.

#### 4.4. Batch Reactions in the Aqueous Phase

For the evaluation of the cofactor regeneration, a double-jacked vessel tempered at 30 °C was used. An amount of 7.5 mM of cinnamyl aldehyde was dissolved in 25 mL potassium phosphate buffer (pH 8, 0.1 M), and the ADH (2 mg) and the FDH (5 mg) were added. The reaction was started by adding 0.1 mM NADH. An amount of 500 µL samples were taken over time, mixed gently with 500 µL xylene and centrifuged. Afterwards, the samples were withdrawn from the upper phase and measured via gas chromatography.

#### 4.5. Investigations via Differential Scanning Fluorimetry

For the investigation, the device Tycho of the company NanoTemper Technologies GmbH (Munich, Germany) was used. The pure compounds were analyzed in potassium phosphate buffer (pH 8, 0.1 M). For the reactions, 25 mL of the buffer were used with 5 mM cinnamyl aldehyde, 100 mM sodium formate, 0.5 mg ADH, 5 mg FDH, and 0.1 mM NADH. For reaction monitoring, samples were taken with a capillary at certain time points, and the first derivatives were plotted against the temperature for investigation of the folding behavior.

#### 4.6. Lab-Scale Cascade

As a first step, the reaction in the aqueous phase was performed in 25 mL potassium phosphate buffer (pH 8, 0.1 mM) at 30 °C. An amount of 5 mM cinnamyl aldehyde was mixed with 2 mg ADH, 5 mg, FDH, 100 mM sodium formate and started with the addition of 0.1 mM NADH. The reaction was monitored via GC until the end of the reaction. Subsequently, the reaction mixture was extracted with 50 mL xylene and the concentration measured via GC. Afterwards, an excess of cinnamic acid (5 mM) was added, as well as 40 mg lipase to start the reaction. This was performed with an overhead stirrer under reflux conditions and a temperature of 60 °C. For reaction monitoring, samples were taken with a syringe via a septum and directly measured via GC.

#### 4.7. Preparation of Silica Particles for Immobilization

For the preparation of the silica particles, a mixture of 1 mol TEOS, 4 mol water, 2.4 mol ethanol, and 10–5 mol HCl was prepared and stirred for 30 min. Afterwards, it was dropped into a mixture of canola oil, butyl amine, and *n*-heptane (890 mL/178 mL/33 mL) via a syringe pump (60 mL syringe, 10 mL/min), and the prepared particles were cured overnight.

For functionalization, 100 g APTES were dissolved in 50 mL ethanol and 10 g particles were incubated at 50 °C for 48 h. The particles were washed with ethanol and stored in water. For cross-linking, the particles were treated with a 2.5% (v/v) glutaraldehyde solution for 1 h at 30 °C and washed afterwards with water for 30 min to remove residual glutaraldehyde. The enzyme immobilization onto the particles was carried out with a solution of 0.5 mg/mL ADH dissolved in phosphate buffer (0.1 M, pH 8), whereby the particles were incubated for 2 h at 25 °C. Subsequently, they were washed with water to remove unbound enzyme.

#### 4.8. Reaction in the Miniplant

A stirred tank reactor containing 800 mL aqueous phase (23.3 mM cinnamaldehyde, 0.1 M phosphate buffer at pH 8.0, 30 °C) is used for the cofactor coupled redox reactions, catalyzed by ADH (21.3 g) and FDH (6.6 g). The organic phase cycle consists of three segments. Cinnamic acid (64 mM) is fed into a reactor of 500 mL containing the organic phase. An extractive centrifuge (CINC CS 50;

Brakel, Deutschland) connects the two cycles, simultaneously mixes the organic and the aqueous phase to extract the intermediate product, and subsequently separates both phases within one apparatus. A fixed bed reactor containing 21 g of immobilized lipase (Novozym<sup>®</sup> 435) is used for the esterification reaction at 60 °C. The total volume of the plant is 5 L [50].

#### 4.9. GC Measurements

A GC 7890A from Agilent Technologies (United States) was used equipped with an FID and an HP-5 column (Agilent Technologies, United States) with helium as carrier gas. For the measurements, 10 µL of the sample were injected with a split of 1:20 and a temperature of 120 °C and analyzed as follows: the temperature was increased from 120 °C with 40 °C/min to 160 °C holding for 2 min, and again, it was increased with 40 °C/min 320 °C holding for 2 min.

**Supplementary Materials:** The following are available online at <http://www.mdpi.com/2073-4344/10/10/1216/s1>.

**Author Contributions:** Conceptualization, C.E. and P.B.; formal analysis, C.E. and J.J.; funding acquisition, T.W. and P.B.; investigation, C.E. and J.J.; project administration, T.W. and P.B.; supervision, G.F. and A.L.; writing—original draft, C.E. and P.B.; writing—review and editing, J.J., T.W., G.F., and A.L. All authors have read and agreed to the published version of the manuscript.

**Funding:** This research was funded by Deutsche Forschungsgemeinschaft: BU3409/1-1 and WA 3957/1-1

**Acknowledgments:** The authors thank Grit Brauckmann, Christina Wallner, as well as Francesca Meyer and Niklas Hartlef for their support in the experimental work.

**Conflicts of Interest:** The authors declare no conflict of interest.

## References

1. Goldberg, K.; Schroer, K.; Lütz, S.; Liese, A. Biocatalytic ketone reduction—A powerful tool for the production of chiral alcohols—Part I: Processes with isolated enzymes. *Appl. Microbiol. Biotechnol.* **2007**, *76*, 237. [CrossRef]
2. Scherkus, C.; Schmidt, S.; Bornscheuer, U.T.; Gröger, H.; Kara, S.; Liese, A. A fed-batch synthetic strategy for a three-step enzymatic synthesis of poly-ε-caprolactone. *ChemCatChem* **2016**, *8*, 3446–3452. [CrossRef]
3. Wu, S.; Snajdrova, R.; Moore, J.C.; Baldenius, K.; Bornscheuer, U. Biocatalysis: Enzymatic Synthesis for Industrial Applications. *Angew. Chem. Int. Ed.* **2020**. [CrossRef] [PubMed]
4. Mali, R.S.; Papalkar, A.S. Synthesis of naturally occurring cinnamyl cinnamates. *J. Chem. Res.* **2001**, *2001*, 433–435. [CrossRef]
5. Demir, A.S.; Talpur, F.N.; Sopaci, S.B.; Kohring, G.-W.; Celik, A. Selective oxidation and reduction reactions with cofactor regeneration mediated by galactitol-, lactate-, and formate dehydrogenases immobilized on magnetic nanoparticles. *J. Biotechnol.* **2011**, *152*, 176–183. [CrossRef]
6. Van Der Donk, W.A.; Zhao, H. Recent developments in pyridine nucleotide regeneration. *Curr. Opin. Biotechnol.* **2003**, *14*, 421–426. [CrossRef]
7. Seelbach, K.; Riebel, B.; Hummel, W.; Kula, M.-R.; Tishkov, V.I.; Egorov, A.M.; Wandrey, C.; Kragl, U. A novel, efficient regenerating method of NADPH using a new formate dehydrogenase. *Tetrahedron Lett.* **1996**, *37*, 1377–1380. [CrossRef]
8. Song, H.; Ma, C.; Liu, P.; You, C.; Lin, J.; Zhu, Z. A hybrid CO<sub>2</sub> electroreduction system mediated by enzyme-cofactor conjugates coupled with Cu nanoparticle-catalyzed cofactor regeneration. *J. CO<sub>2</sub> Util.* **2019**, *34*, 568–575. [CrossRef]
9. Han, L.; Liang, B. New approaches to NAD(P)H regeneration in the biosynthesis systems. *World J. Microbiol. Biotechnol.* **2018**, *34*, 141. [CrossRef]
10. Wang, X.; Saba, T.; Yiu, H.H.; Howe, R.F.; Anderson, J.A.; Shi, J. Cofactor NAD (P) H regeneration inspired by heterogeneous pathways. *Chem* **2017**, *2*, 621–654. [CrossRef]
11. Aslan, A.S.; Valjakka, J.; Ruuponen, J.; Yildirim, D.; Turner, N.J.; Turunen, O.; Binay, B. *Chaetomium thermophilum* formate dehydrogenase has high activity in the reduction of hydrogen carbonate (HCO<sub>3</sub><sup>-</sup>) to formate. *Protein Eng. Des. Select. PEDS* **2017**, *30*, 47–55.

12. Pennacchio, A.; Rossi, M.; Raia, C.A. Synthesis of cinnamyl alcohol from cinnamaldehyde with *Bacillus stearothermophilus* alcohol dehydrogenase as the isolated enzyme and in recombinant *E. coli* cells. *Appl. Biochem. Biotechnol.* **2013**, *170*, 1482–1490. [\[CrossRef\]](#) [\[PubMed\]](#)
13. Cocchiara, J.; Letizia, C.; Lalko, J.; Lapczynski, A.; Api, A. Fragrance material review on cinnamaldehyde. *Food Chem. Toxicol.* **2005**, *43*, 867–923. [\[CrossRef\]](#) [\[PubMed\]](#)
14. Vitolo, M.; Yoriyaz, E.J. Reduction of prochiral ketones by NAD (H)-dependent alcohol dehydrogenase in membrane reactor. *Athens J. Sci.* **2015**, *2*, 161–175. [\[CrossRef\]](#)
15. Marpani, F.; Sárossy, Z.; Pinelo, M.; Meyer, A.S. Kinetics based reaction optimization of enzyme catalyzed reduction of formaldehyde to methanol with synchronous cofactor regeneration. *Biotechnol. Bioeng.* **2017**, *114*, 2762–2770. [\[CrossRef\]](#)
16. Mee, B.; Kelleher, D.; Frias, J.; Malone, R.; Tipton, K.F.; Henehan, G.T.; Windle, H.J. Characterization of cinnamyl alcohol dehydrogenase of *Helicobacter pylori*: An aldehyde dismutating enzyme. *FEBS J.* **2005**, *272*, 1255–1264. [\[CrossRef\]](#)
17. Kroutil, W.; Mang, H.; Edegger, K.; Faber, K. Biocatalytic oxidation of primary and secondary alcohols. *Adv. Synth. Catal.* **2004**, *346*, 125–142. [\[CrossRef\]](#)
18. Liese, A.; Seelbach, K.; Wandrey, C. *Industrial Biotransformations*; John Wiley & Sons: Hoboken, NJ, USA, 2006.
19. Ansorge-Schumacher, M.B.; Slusarczyk, H.; Schümers, J.; Hirtz, D. Directed evolution of formate dehydrogenase from *Candida boidinii* for improved stability during entrapment in polyacrylamide. *FEBS J.* **2006**, *273*, 3938–3945. [\[CrossRef\]](#)
20. Weckbecker, A.; Hummel, W. Improved synthesis of chiral alcohols with *Escherichia coli* cells co-expressing pyridine nucleotide transhydrogenase, NADP<sup>+</sup>-dependent alcohol dehydrogenase and NAD<sup>+</sup>-dependent formate dehydrogenase. *Biotechnol. Lett.* **2004**, *26*, 1739–1744. [\[CrossRef\]](#)
21. Schirwitz, K.; Schmidt, A.; Lamzin, V.S. High-resolution structures of formate dehydrogenase from *Candida boidinii*. *Protein Sci.* **2007**, *16*, 1146–1156. [\[CrossRef\]](#)
22. Garcia, T.; Coteron, A.; Martinez, M.; Aracil, J. Kinetic modelling of esterification reactions catalysed by immobilized lipases. *Chem. Eng. Sci.* **1996**, *51*, 2841–2846. [\[CrossRef\]](#)
23. Fjerbaek, L.; Christensen, K.V.; Norddahl, B. A review of the current state of biodiesel production using enzymatic transesterification. *Biotechnol. Bioeng.* **2009**, *102*, 1298–1315. [\[CrossRef\]](#) [\[PubMed\]](#)
24. Wierschem, M.; Schlimper, S.; Heils, R.; Smirnova, I.; Kiss, A.A.; Skiborowski, M.; Lutze, P. Pilot-scale validation of enzymatic reactive distillation for butyl butyrate production. *Chem. Eng. J.* **2017**, *312*, 106–117. [\[CrossRef\]](#)
25. Bansode, S.R.; Hardikar, M.A.; Rathod, V.K. Evaluation of reaction parameters and kinetic modelling for Novozym 435 catalysed synthesis of isoamyl butyrate. *J. Chem. Technol. Biotechnol.* **2017**, *92*, 1306–1314. [\[CrossRef\]](#)
26. Heinsman, N.W.; Valente, A.M.; Smienk, H.G.; van der Padt, A.; Franssen, M.C.; de Groot, A.; van 't Riet, K. The effect of ethanol on the kinetics of lipase-mediated enantioselective esterification of 4-methyloctanoic acid and the hydrolysis of its ethyl ester. *Biotechnol. Bioeng.* **2001**, *76*, 193–199. [\[CrossRef\]](#)
27. Yadav, G.D.; Borkar, I.V. Synthesis of n-butyl acetamide over immobilized lipase. *J. Chem. Technol. Biotechnol. Int. Res. Process Environ. Clean Technol.* **2009**, *84*, 420–426. [\[CrossRef\]](#)
28. Yadav, G.D.; Dhoot, S.B. Immobilized lipase-catalysed synthesis of cinnamyl laurate in non-aqueous media. *J. Mol. Catal. B Enzym.* **2009**, *57*, 34–39. [\[CrossRef\]](#)
29. Wang, Y.; Jiang, Y.; Zhou, L.; Gao, J. Enzymatic esterification of ammonium lactate with ethanol in organic solvent: Kinetic study. In Proceedings of the 2010 4th International Conference on Bioinformatics and Biomedical Engineering, Chengdu, China, 18–20 June 2010; IEEE: Piscataway, NJ, USA, 2010; pp. 1–4.
30. Miguel, V.; Trubiano, G.; Perez, G.; Borio, D.; Errazu, A. Kinetic analysis of enzymatic esterification of fatty acids and ethanol. In *Studies in Surface Science and Catalysis*; Elsevier: Amsterdam, The Netherlands, 2001; Volume 133, pp. 619–624.
31. Ganapati, D.; Yadav, K.; Manjula, D. Immobilization lipase-catalysed esterification and transesterification reactions in non-aqueous media for the synthesis of tetrahydrofurfuryl butyrate: Comparison and kinetic modeling. *Chem. Eng. Sci.* **2004**, *59*, 373–383.
32. Straathof, A. Development of a computer program for analysis of enzyme kinetics by progress curve fitting. *J. Mol. Catal. B Enzym.* **2001**, *11*, 991–998. [\[CrossRef\]](#)
33. Duggleby, R.G.; Morrison, J.F. Progress curve analysis in enzyme kinetics. Model discrimination and parameter estimation. *Biochim. Biophys. Acta (BBA) Enzymol.* **1978**, *526*, 398–409. [\[CrossRef\]](#)

34. Shinde, S.D.; Yadav, G.D. Insight into microwave-assisted lipase catalyzed synthesis of geranyl cinnamate: Optimization and kinetic modeling. *Appl. Biochem. Biotechnol.* **2015**, *175*, 2035–2049. [CrossRef] [PubMed]
35. Geng, B.; Wang, M.; Qi, W.; Su, R.; He, Z. Cinnamyl acetate synthesis by lipase-catalyzed transesterification in a solvent-free system. *Biotechnol. Appl. Biochem.* **2012**, *59*, 270–275. [CrossRef] [PubMed]
36. Alfonsi, K.; Colberg, J.; Dunn, P.J.; Fevig, T.; Jennings, S.; Johnson, T.A.; Kleine, H.P.; Knight, C.; Nagy, M.A.; Perry, D.A. Green chemistry tools to influence a medicinal chemistry and research chemistry based organisation. *Green Chem.* **2008**, *10*, 31–36. [CrossRef]
37. Bes, M.T. Gomez-Moreno, C.; Guisan, J.M. Fernandez-Lafuente, R. Selective oxidation: Stabilisation by multipoint attachment of ferredoxin NADP+ reductase, an interesting cofactor recycling enzyme. *J. Mol. Catal. A Chem.* **1995**, *98*, 161–169. [CrossRef]
38. Stepankova, V.; Bidmanova, S.; Koudelakova, T.; Prokop, Z.; Chaloupkova, R.; Damborsky, J. Strategies for stabilization of enzymes in organic solvents. *ACS Catal.* **2013**, *3*, 2823–2836. [CrossRef]
39. Straathof, A. Auxiliary phase guidelines for microbial biotransformations of toxic substrate into toxic product. *Biotechnol. Prog.* **2003**, *19*, 755–762. [CrossRef]
40. Grundtvig, I.P.R.; Heintz, S.; Krühne, U.; Gernaey, K.V.; Adlercreutz, P.; Hayler, J.D.; Wells, A.S.; Woodley, J.M. Screening of organic solvents for bioprocesses using aqueous-organic two-phase systems. *Biotechnol. Adv.* **2018**, *36*, 1801–1814. [CrossRef]
41. Laane, C.; Boeren, S.; Vos, K.; Veeger, C. Rules for optimization of biocatalysis in organic solvents. *Biotechnol. Bioeng.* **1987**, *30*, 81–87. [CrossRef]
42. Cantarella, L.; Alfani, F.; Cantarella, M. Stability and activity of immobilized hydrolytic enzymes in two-liquid-phase systems: Acid phosphatase,  $\beta$ -glucosidase, and  $\beta$ -fructofuranosidase entrapped in poly (2-hydroxyethyl methacrylate) matrices. *Enzym. Microb. Technol.* **1993**, *15*, 861–867. [CrossRef]
43. Ansorge-Schumacher, M.B.; Steinsiek, S.; Eberhard, W.; Keramidas, N.; Erkens, K.; Hartmeier, W.; Büchs, J. Assaying CO<sub>2</sub> release for determination of formate dehydrogenase activity in entrapment matrices and aqueous-organic two-phase systems. *Biotechnol. Bioeng.* **2006**, *95*, 199–203. [CrossRef]
44. Duan, Z.; Sun, R. An improved model calculating CO<sub>2</sub> solubility in pure water and aqueous NaCl solutions from 273 to 533 K and from 0 to 2000 bar. *Chem. Geol.* **2003**, *193*, 257–271. [CrossRef]
45. Bommarius, A.S.; Paye, M.F. Stabilizing biocatalysts. *Chem. Soc. Rev.* **2013**, *42*, 6534–6565. [CrossRef] [PubMed]
46. Bommarius, A.S.; Karau, A. Deactivation of formate dehydrogenase (FDH) in solution and at gas-liquid interfaces. *Biotechnol. Prog.* **2005**, *21*, 1663–1672. [CrossRef] [PubMed]
47. Hartlef, N. *Experimentelle Charakterisierung und Computergestützte Modellierung Enzymatisch Katalysierter RedOx-Reaktionen*; Hamburg University of Technology: Hamburg, Germany, 2019.
48. Orlich, B.; Schomaeker, R. Enzymatic reduction of a less water-soluble ketone in reverse micelles with nadh regeneration. *Biotechnol. Bioeng.* **1999**, *65*, 357–362. [CrossRef]
49. Gröger, H.; Hummel, W.; Rollmann, C.; Chamouleau, F.; Hüsken, H.; Werner, H.; Wunderlich, C.; Abokitse, K.; Drauz, K.; Buchholz, S. Preparative asymmetric reduction of ketones in a biphasic medium with an (S)-alcohol dehydrogenase under in situ-cofactor-recycling with a formate dehydrogenase. *Tetrahedron* **2004**, *60*, 633–640. [CrossRef]
50. Johannsen, J.; Engelmann, C.; Liese, A.; Fieg, G.; Bubenheim, P.; Waluga, T. Pilot-scale Operation of a Multi-enzymatic Cascade Reaction in a Multiphase System. *Chem. Eng. Trans.* **2020**, *79*, 25–30.
51. Engelmann, C.; Ekambaram, N.; Johannsen, J.; Fellechner, O.; Waluga, T.; Fieg, G.; Liese, A.; Bubenheim, P. Enzyme Immobilization on Synthesized Nanoporous Silica Particles and their Application in a Bi-enzymatic Reaction. *ChemCatChem* **2020**, *12*, 2245–2252. [CrossRef]

**Publisher's Note:** MDPI stays neutral with regard to jurisdictional claims in published maps and institutional affiliations.



© 2020 by the authors. Licensee MDPI, Basel, Switzerland. This article is an open access article distributed under the terms and conditions of the Creative Commons Attribution (CC BY) license (<http://creativecommons.org/licenses/by/4.0/>).